44TH TURBOMACHINERY & 31ST PUMP SYMPOSIA
HOUSTON, TEXAS | SEPTEMBER 14 – 17 2015
GEORGE R. BROWN CONVENTION CENTER

# APPLYING CFD TO SOLVE A VIBRATION PROBLEM OF A COMPRESSOR

**Roberto F. de Noronha, Ph.D.**
Petróleo Brasileiro S.A. - PETROBRAS
Rio de Janeiro, RJ, BRASIL
+55 21 3876 7439
roberto.noronha@petrobras.com.br

**Letícia de Rezende Tapajóz**
Petrobras Research Center - CENPES
Rio de Janeiro, RJ, BRASIL
+55 21 2162 1250
tapajoz@petrobras.com.br

**Glenn R. Grosso**
Dresser-Rand Company
Olean, NY
716-375-3359
ggrosso@dresser-rand.com

**Diogo Yoshikazu Ujihara, MSc.**
Petróleo Brasileiro S.A. - PETROBRAS
Rio de Janeiro, RJ, BRASIL
+55 21 3876 4173
ujihara.HOPE@petrobras.com.br

**Rodrigo Peralta Muniz Moreira**
Engineering Simulation and Scientific Software - ESSS
Rio de Janeiro, RJ, BRASIL
+55 21 2162 2495
peralta@esss.com.br

*Dr. Roberto Noronha is with Petrobras since 2005 as a Rotating Equipment Advisor at the Rio de Janeiro Operation Unit, providing vibration advice for its eleven production platforms. He was previously with Fluminense Federal University as an Associate Professor. He received his BSc degree (Mechanical Engineering) from Catholic University of Rio de Janeiro, MSc. degree from Federal University of Paraiba and a UK PhD degree from Cranfield University.*

*Leticia de Rezende Tapajoz is a research engineer of Petrobras Research and Development Center (CENPES) since 2010. She is currently responsible for upstream equipment research and technology, including turbomachinery. She received her BSc degree in Mechanical Engineering in 2010 from Federal University of Rio de Janeiro.*

*Glenn Grosso is the Manager of Centrifugal Products Technical Support for Dresser-Rand Turbo Products and a Dresser-Rand Engineering Fellow. He has 36 years of design experience on rotary screw, axial flow, and centrifugal compressors. He graduated with a BSME degree from Rutgers University College of Engineering. He is a licensed Professional Engineer in the state of New Jersey.*

*Diogo Yoshikazu Ujihara works as a rotordynamics specialist at Petrobras since 2011. He received his BSc degree in Mechanical Engineering from Fluminense Federal University (2008) and a MSc. degree from the same university in 2011.*

*Rodrigo Peralta Muniz Moreira received his BSc degree (Chemical Engineer) from Federal University of Santa Catarina (UFSC) in 2012 and is currently studying for M.Sc. degree in Federal University of Rio de Janeiro (UFRJ) at COPPE Chemical Engineering Program. He works at ESSS since 2009 as CAE Applications Specialist.*

## ABSTRACT

This paper presents an application of CFD on solving a compressor vibration problem. The numerical technique was used to calculate the dynamical coefficients of a damper seal with a hybrid hole-pattern - labyrinth configuration, which leads to some difficulties when employing the usual bulk flow based applications.

## INTRODUCTION

Gas annular seals are widely used to reduce internal leakage in turbomachinery. The fluid flows from a high pressure to a low-pressure region, generating dynamic forces that may affect the behavior of the machine. Therefore, depending on the type of analysis or the size of the dynamic forces, the dynamic coefficients of the annular seals may need to be included when preparing a rotordynamic model.

The software most used by OEMs and operators to predict those coefficients are based on bulk flow theory, which uses empirical friction factors. Even though friction factors have been through many experimental validations, they can still lead to some inaccuracies. Those simplifications are not necessary if a full computational fluid dynamics (CFD) analysis is made. Hence, CFD has been successfully employed for the development and improvement of annular seals. However, taking into account the increased availability of numerical processing, it may be also used in problem solving, as discussed in the following example.

A persistent vibration issue in some of the operator's centrifugal compressors was identified as being caused by the balance piston damper seal providing excessive stiffness. Therefore, a modification on the geometry of the balance piston and seal was required. The approach was to calculate a new geometry for this set and perform rotordynamic simulations to ensure that the rotor to be installed would vibrate less than the one in operation.

Since the seal has a hybrid configuration, part labyrinth, part hole-pattern, as discussed further in the text, the usual programs for seal modeling would produce some inaccuracies, since whirl ratio and pressure between the two types of seals were unknown. Furthermore, good accuracy in the calculation of the seal coefficients is required because if they were underestimated, the observed behavior of the rotor would persist, but instability could take place if the damping coefficients were less than predicted. Therefore, it was decided to use CFD to calculate the damper seal coefficients. This paper presents the methodology used to redesign this gas annular damper seal and solve the vibration issue, employing CFD together with the rotordynamic analysis.

## PROBLEM DESCRIPTION

The issue took place on a FPSO unit with capacity of 180 thousand bpd of oil located on the Campos Basin, offshore the Brazilian coast. The compression plant is composed of three compressor trains driven by variable speed electric motors via VSD, each train consisting of a back-to-back LP compressor and a straight-through HP one, with nominal capacity of two million standard cubic meters per train and 200 barg discharge pressure.

In January 2012, the spare rotor of the HP compressors was installed on one train, presenting high vibration from the beginning of the operation. The figure below, which refers to one of the non-drive end, NDE, sensors during a cold start-up, is representative of the problem. The colors blue, orange and red represent, respectively, the vibration filtered at the frequency of rotation, called 1X vibration (with amplitude below and phase angle on top), the overall vibration, and rotation itself. In the first 30 minutes, including startup and passage through the critical speed, the overall vibration is around 20 microns (amplitude scale on the right side of the plot). This was true for all four sensors, indicating a well-balanced rotor. Next, the 1X vibration amplitude increases, pushing together the overall vibration, and a steep change on the phase angle occurs. This takes place on the two NDE sensors and characterizes a change in the stiffness of the system, causing an increase in sensitivity to unbalance on the non-drive end. Correlation of the vibration signals with process data confirmed that the increase in vibration was caused by the closure of the recycle valve. It led to a change on the dynamics of the system, pushing the first critical speed into the operation range. As discussed next, the mode shape for this new first critical would be similar to a cantilever, with the NDE side "free".

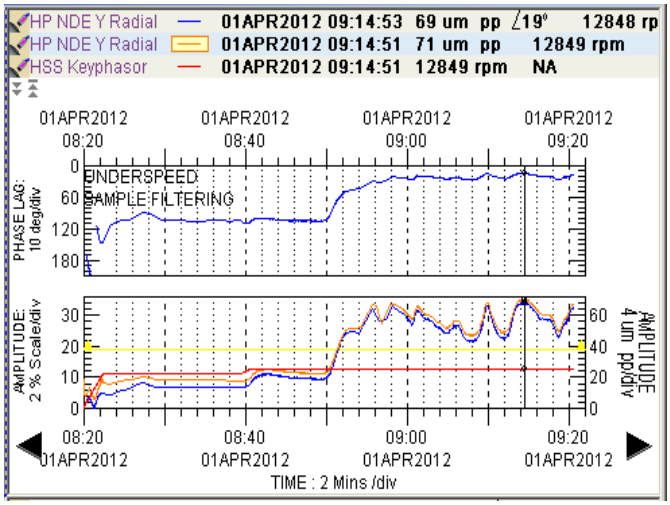

Figure 1 – April 1st Start up – Sensor NDE Y: overall vibration in orange; 1X filtered in blue; speed in red.

The use of squeeze film dampers around the bearings and damper seal of the type hole-pattern on the balance piston located near the drive end, DE, of the compressor are design features of this straight through compressor. Both components are designed to increase the damping of the rotor to ensure greater stability. However, while the squeeze film dampers reduce the stiffness of the bearings, the damper seal introduces additional stiffness on the drive end, leaving the NDE more susceptible to vibration, similar to a cantilever beam. This

effect is a function of the degree of closure of the recycle valve. This is because the stiffness and damping introduced by this seal are function of the gas leakage through the seal, which is in turn a function of the pressure difference between the compressor suction and discharge.

The manufacturer had proposed a series of changes in rotor design to reduce this susceptibility in 2006, when the platform began oil production, including replacement of the full hole-pattern seal for a hybrid solution, with part in labyrinth, as shown in figure 2. Even so, a higher vibration on the NDE occurred on the nine similar compressors installed on the Campos Basin platforms. The conclusion of the vibration behavior of this particular compressor was that it was due to the combination of the diametric dimensions of the balance piston and its seal, which led to high stiffness when pressure gradient was maximized by recycle valve closure.

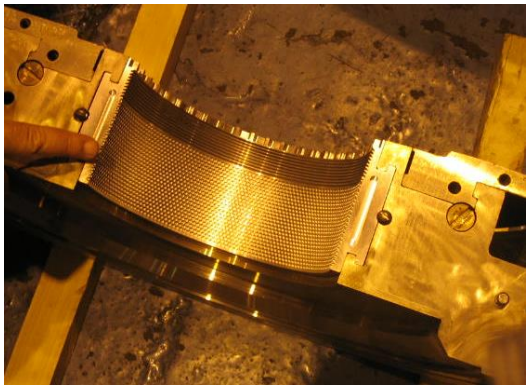

Figure 2 – Hybrid Seal

## SEAL CLEARANCE ANALYSIS

An important parameter for damper seals is the convergence ratio of the annular gap between piston and seal. If convergent, the seal produces a positive stiffness while if divergent, the stiffness is negative. According to the quality control done before mating the rotor with the compressor bundle, the clearances of the damper seals of these compressors are convergent, and the measured clearances along three axial positions were within specified limits. Nevertheless, as discussed in a following section, a comparison between two rotordynamic simulations, one considering damper seal effects and the other neglecting it, showed increased sensitivity to unbalance at the NDE sensor.

Since the seal is hybrid, the wearing out of the labyrinth seal leads to an increase of the pressure difference and leakage across the damper seal, increasing its stiffness contribution. This is what happened over 16 months, with the NDE vibration rising until it was not possible to load completely the compressor, because as the recycle valve closed, the vibration rose. Mitigation actions, like bearing swaps and realignment were tried without success, up to the point that it was not possible to postpone a new rotor change.

Before doing this change, using the records of clearance of the actual running and of the new spare rotor & bundle set, stiffness and damping coefficients were calculated using a rotordynamic software package (XLTRC2, 2015) for both seal cases. The conclusion was that the damper seal of the spare set would produce higher stiffness than the one in operation, as shown at Table 3, columns “rotor in operation” and “without modification”. Therefore, if the damper seal was used without modifications, it would produce a behavior as bad as or worse than the one that was in operation.

It was necessary to change the geometry of the set to minimize this effect. At the operator side, the adopted approach was to calculate a new configuration of the balance piston, taking into account clearance and taper, and perform damped unbalance response and stability analyses, to ensure that, after changing the rotors, the new one would vibrate less than the one in operation. In order to accomplish this, it was necessary to consider that:

- Initially, for these simulations, it is necessary to determine the stiffness and damping coefficients of the annular seals, which is still imprecise. A survey from Kocur, et al. (2007), points out to high variations in these results. This difficulty is increased by the fact that the subject seal is a hybrid type, with a portion being labyrinth.
- On the other hand, the precision in the calculation of these coefficients is necessary, because if they become too high, it would lead to the already observed behavior of the rotor. Should they become too small, it could lead to instability.
- Therefore the participation of the manufacturer was very important since he would have more experience and greater awareness of the limitations of the annular seal software based on bulk flow theory.
- However, given the gas and oil losses that were occurring at the platform, it was necessary to seek in parallel an alternative solution, since the response from the manufacturer could take a long time. This alternative solution was in three stages: First, seek for a better geometry configuration of the balance piston using standard bulk flow theory based software, recalculate the dynamic coefficients through CFD and confirm the results through rotordynamic simulations.

In mid-May 2013, a new balance piston configuration arose which was expected to produce a reduction in stiffness without significant changes in damping. In Figure 3 sketches of

the balance piston of the spare rotor are presented, without and with modifications. The considered dimensions for the new balance piston are different from the configuration that the OEM considered as original configuration, discussed in the next section. The stiffness and damping coefficients calculated with the rotordynamic code for the rotor in operation, for the spare rotor without modification and for the modified balance piston are presented at Table 3.

Two weeks later, with the CFD analyses already started, the manufacturer presented another modification proposal, which was also included in the analyses.

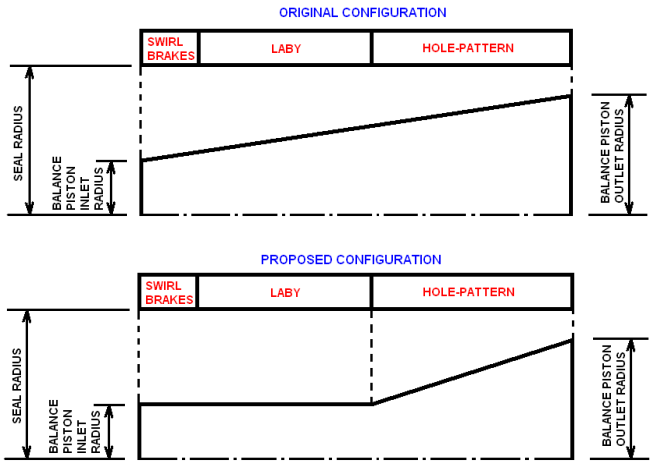


Figure 3 - Proposed Modification on Balance Piston – correspond to cases A and B in the CFD simulations.

## DESIGN MODIFICATION FROM THE MANUFACTURER

The HP compressor under discussion is a straight-through, 8-stage compressor with a 24" case bore with the thrust bearing located at the suction (non-drive) end and the balance piston located at the discharge (drive) end of the compressor.

Due to the urgent need for a resolution and the difficulty that can often occur with moving parts across international borders, an investigation into potential modifications of the existing balance piston seal(s) in Brazil was undertaken by the OEM. The analysis technique was more traditional in nature, that being to use the ISOTSEAL damper seal code (Kleynhans and Childs, 1997) in conjunction with the OEM rotordynamic codes. The seal, as noted earlier, is a hybrid seal design consisting of a convergent hole-pattern seal section at the low pressure side, combined with a straight diameter labyrinth tooth section (with inlet swirl breaks) at the high pressure entrance to the seal. The use of this seal type was determined from factory full-load, full-pressure and hydrocarbon testing when the compressor train was originally tested years ago. A reduction in the seal effects when under load while maintaining the same balance piston overall leakage rate was the driving factor in the original application of the hybrid seal at the balance piston location.

Seal stiffness and damping rotordynamic coefficients for the balance piston damper seal and labyrinth seal portion were determined based on field aerodynamic performance data obtained in conjunction with field vibration data. The synchronous forced response analysis was run both with and without the balance piston seal data included in the rotor model. Field vibration data suggested low overall vibration levels when the units reached speed. The vibration level increase was not simply a transient phenomenon, but remained high at the thrust end once the HP compressor was loaded. What was being experienced were end states of two separate steady-state operating conditions. Since the damper seal requires differential pressure to develop significant stiffness and damping characteristics, a comparison of the rotordynamic results from a bearings-only analysis were compared, as the baseline, to the results of rotordynamic analyses inclusive of the damper seal effects at load. All the reported vibration was synchronous with no sub-synchronous components of concern observed. Basis this information, it was determined that comparisons of the unbalance sensitivity values from the forced response analyses was the best information to use to determine the effectiveness of possible modifications.

Several potential seal modification paths were reviewed. The goals of the modifications were to:

(1) Reduce the synchronous vibration levels at the thrust end
(2) Maintain adequate rotor stability
(3) Minimize the increase in balance piston seal leakage rate and
(4) Make the rework simple and avoid complicated machining work that could be difficult to complete in the field.

The path chosen here was to remove material that did the least amount of good from a leakage standpoint while effectively reducing the stiffness and damping coefficients. Thus, the modifications focused on removing material from the inlet area of the hole-pattern section of the seal, since that area had the largest clearance to the balance piston surface.

With the path defined, sensitivity values were plotted for several potential lengths of material removal from the large clearance (upstream) end of the hole-pattern seal section. A tabulation of the sensitivity values obtained is shown in Table 1 below:

**Table 1** – Unbalance Sensitivity Values for Various Analytical Runs

| Run # | Analysis and Modification Description (all runs made using a mid-span unbalance configuration) | Thrust End Minimum Brg Clr and Oil Temp (mils per ounce-inch @MCS) | Non-Thrust End Minimum Brg Clr and Oil Temp (mils per ounce-inch @ MCS) | Thrust End Maximum Brg Clr and Oil Temp (mils per ounce-inch @ MCS) | Non-Thrust End Maximum Brg Clr and Oil Temp (mils per ounce-inch @MCS) | Balance Piston Hybrid Seal Configuration Nominal Calculated Leakage (kg/s) |
|---|---|---|---|---|---|---|
| 1 | Synchronous Forced Response Analysis with NO Seal Effects Included | 0.127 | 0.126 | 0.390 | 0.368 | 1.04 |
| 2 | Synchronous Forced Response Analysis with Existing Hybrid Laby-Hole Pattern Seal Effects Included | 0.184 | 0.099 | 0.517 | 0.259 | 1.04 |
| 3 | Synchronous Forced Response Analysis with Modified Hole Pattern Seal - 0.5" Hole Pattern Removal from LP End of Seal | 0.165 | 0.107 | 0.473 | 0.295 | 1.22 |
| 4 | Synchronous Forced Response Analysis with Modified Hole pattern Seal - 1.0" Hole Pattern Removal from the HP End of Seal | 0.156 | 0.110 | 0.453 | 0.312 | 1.24 |
| 5 | Synchronous Forced Response Analysis with Modified Hole Pattern Seal - 1.38" Hole Pattern Removal from the HP End of Seal | 0.148 | 0.114 | 0.434 | 0.327 | 1.25 |

Table 1 has a lot of information in it. The results of five analytical runs are shown. The first run represents the sensitivities of the rotor model without any damper seal effects included. This run was considered the baseline run, representative of the rotor in the field at the time when it first reached speed, but with the recycle valves fully open, meaning the compressor generated the least amount of differential pressure. The second run is the forced response run made inclusive of damper seal coefficients (determined at original design conditions), and applied at the balance piston location. This run represents the rotor in the field after the recycle valves are closed and operating at steady-state conditions online in the process. The difference in the predicted sensitivity to unbalance at the thrust end and non-thrust end locations between the first and second run represents the expected change in machine vibration levels at each location. You will note that the inclusion of the damper seal coefficients results in reduced expected synchronous vibration levels at the non-thrust end (end closest to the balance piston). It also predicts that the synchronous vibration levels will increase when the compressor recycle valves are closed at the thrust end of the compressor. This predicted change in sensitivity between the second and first runs matches the observed field behavior well at the thrust end. This "sensitivity band" became the basis to use to gage the effects of potential seal modifications. The green and yellow cells in Table 1 were then the primary rotordynamic program outputs that were focused on. As will be discussed in a plot later on, the effort was being made to increase the margin to the first critical speed of the compressor when damper seal effects are included.

As noted earlier, and to be discussed in more detail later, one of the concerns of the analytical work is related to the estimation of the inlet swirl of the process gas entering the damper seal. This is in large part because the source of that gas is the exit swirl out of the upstream labyrinth tooth section plus additional swirl potential developed in the clearance space between the seals. While the axial clearance space between the labyrinth and hole-pattern seal sections is small on the original seal as shown in Figure 2, the modification plans to be discussed further on included a significant increase in that distance.

Due to the urgency required here, the method used by the OEM to estimate the entrance swirl to the hole-pattern seal was a combination of engineering judgment and a quick comparative study using the damper seal code noted earlier. The comparative study was performed to review the effect on the direct and cross-coupled stiffness and damping values from the damper seal code with the only variable changing being the inlet swirl ratio to the damper seal. Results of that study, which are based on the original length hole-pattern seal as shown in Figure 2, are presented in Figure 4 and Figure 5 below.

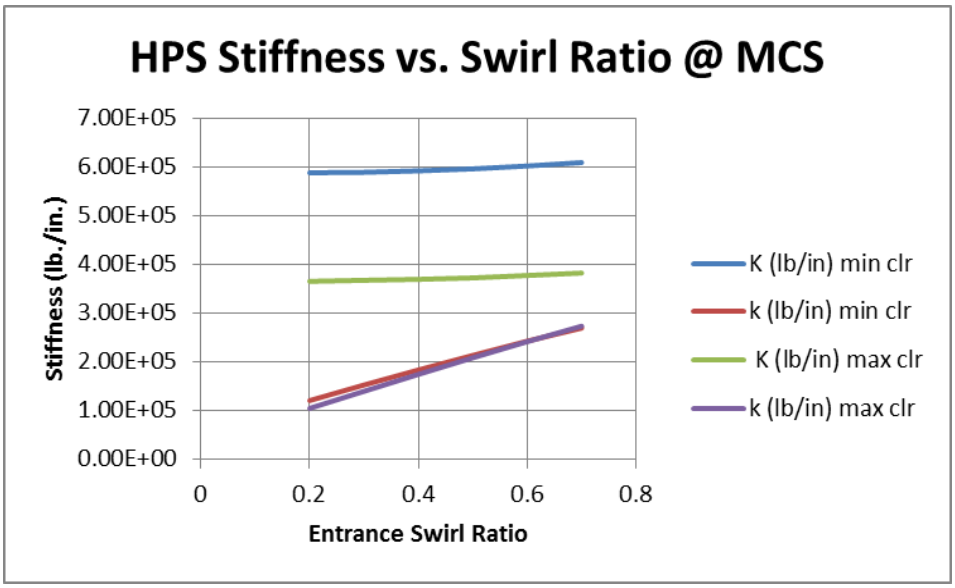


Figure 4 – Direct (K) and Cross-Coupled (k) Stiffness versus Swirl Ratio

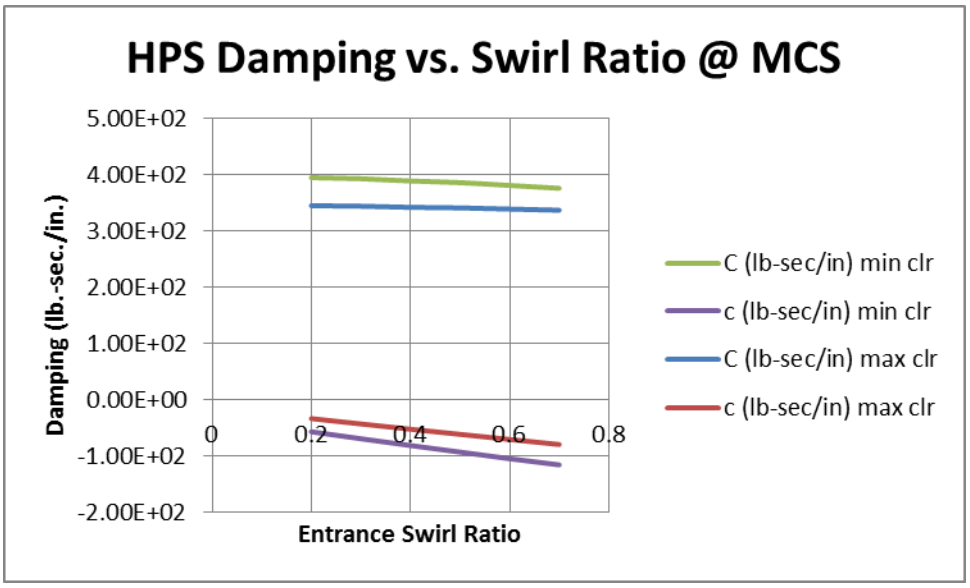


Figure 5 – Direct (C) and Cross-Coupled (c) Damping versus Swirl Ratio

Of interest here it can be noted that for swirl ratios between 0.2 and 0.7 the damper seal code predicts very small differences (less than 10%) in direct stiffness or in direct damping. There are much more substantial changes in the cross-coupled stiffness and cross-coupled damping values over that same swirl ratio range. Even here, however, given a reasonable estimation of where the swirl ratio would be expected to fall, being off by +/- 0.1, or even +/- 0.2, suggests that the results obtained should provide suitable accuracy for diagnostic purposes. The damper seal modification analysis work performed by the OEM was basis an inlet swirl ratio of 0.6.

Returning to Table 1, runs 3, 4, and 5 (all based on run 2 operating conditions) are labeled by the amount of material removed from the existing hole-pattern seal section and which end it was removed from. Run 3 had material removed from the close clearance (low pressure) end of the hole-pattern while runs 4 and 5 had different amounts of material removed from the larger clearance (high pressure) end of the hole-pattern seal.

Runs 3, 4, and 5 had similar overall leakage increases, as listed in Table 1, of approximately 20% over the current balance piston design, which was deemed acceptable aerodynamically. It can be seen from the sensitivity values in runs 3, 4, and 5 that varying the length of the damper seal, and from which end, has an impact on the forced response results. The two values highlighted in yellow in run two were the "current state" sensitivity values of the loaded HP compressor based on a mid-span unbalance distributions. In our experience, most beam-style centrifugal compressors vibrate with a tendency that suggests mid-span unbalance distributions predominate. Using the mid-span unbalance configuration as the primary source for comparative values, runs 3, 4, and 5 were compared against each other and also to resulting sensitivity values at each end. It can be seen that between runs 1 and 2 that the sensitivity at minimum conditions at the thrust end increases 45% between no-seal/seal effects, and about 32% at maximum conditions. Also the TE (thrust end) versus NTE (non-thrust end) comparisons suggest the TE has an 85 – 99% higher sensitivity to unbalance than the NTE with seal effects included. This is as opposed to the original run one where the sensitivity values (again all mid-span based) were well within 10% of each other. After several iterations run 5 was chosen as the best compromise. It reduced the thrust end sensitivities, inclusive of modified damper seal effects, to within 15% of the no-seal-effects run based on mid-span unbalance configurations. Run five also resulted in the end-to-end sensitivity differences being within approximately 30% of each other.

The modification configuration chosen was then confirmed to maintain adequate rotor stability. OEM stability programs were run using the OEM method for calculating the anticipated rotor cross-coupling and the log decrement values changed from 0.72 to 0.61 at minimum clearance, indicating acceptable rotor stability had been maintained.

As noted in the four goals above, the last step was to ensure the seal modification was simple enough to permit re-machining efforts in the field to be successful. The resulting modification was simply the machining of a relief pocket diameter behind the laby tooth portion of the hybrid seal to an adequate depth to remove the hole-pattern for the distance determined by the analysis. This pocket depth was not a critical parameter and the modification was easily performed on an engine lathe in the field. No other modifications were required to be made.

## CFD SIMULATIONS

As discussed in the Introduction, currently, two methods are used: bulk flow analysis and computational fluid dynamics (CFD). Bulk flow methods use the lubricant films theory developed by Hirs (1973) in one or two control volumes, neglecting velocity fluctuations due to turbulence and the shape of the velocity profile in favor of bulk mean fluid flow variables (Migliorini, 2012). Additionally, the wall shear stresses are described in terms of the bulk mean fluid velocity through empirical coefficients (friction factors). Making these assumptions the governing equations are simplified, reducing the computational time required for the analysis of lubricant films (Hirs, 1973, and Childs, 1993). Many numerical, experimental and analytical studies have been conducted to validate those methods, but only experimental measurement of each seal could get more accurate results (Migliorini, 2012).

CFD analyses eliminate the use of the empirical coefficients since the wall shear stress is determined at a highly detailed level in the solution. Therefore, the use of CFD to obtain the rotordynamic coefficients of annular seals has been the focus of many studies.

Yan et al. (2011) used CFD to determine the rotordynamic coefficients of a hole-pattern seal, assuming a periodic circular orbit of the rotor, as described by Eq. (1). The transient solution combined with mesh deformation, as used by Chochua and Soulas (2007), was adopted to solve the leakage flow field.

$$\begin{aligned} x &= r\cos(\Omega t) \\ y &= r\sin(\Omega t) \\ z &= 0 \end{aligned} \tag{1}$$

*Numerical Model and Operating Conditions*

Since the seal has a nonaxisymmetric geometry and off centered rotation, the full circumferential model (360 deg) was necessary. Three different configurations of the damper seal were simulated. The first one, named Case A, has the geometry of the spare damper seal available at the operator`s turbomachinery workshop and is shown in Fig. 6. Case B considers the same configuration of case A for the damper seal, with a slight modification on the balance piston geometry, as illustrated in Fig. 3. Finally, Case C has the geometry of the damper seal with the modifications presented by the manufacturer. This last configuration can be seen in Fig. 7. Note that the models presented in both figures 6 and 7 show the region of the gas between the surfaces of the piston and the seal, as required for CFD simulations.

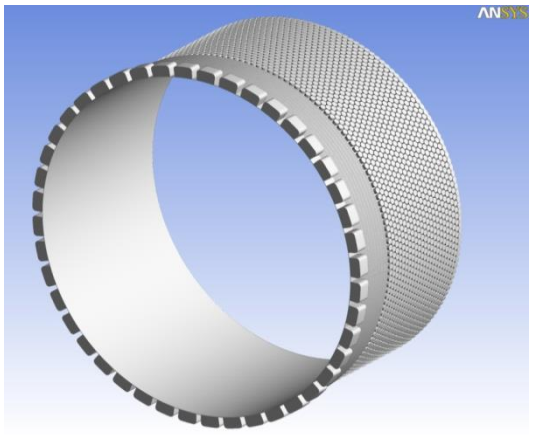

Figure 6 – Case A computational model.

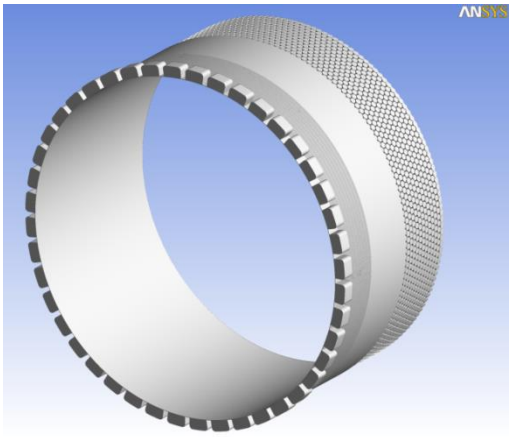

Figure 7 – Case C computational model.

A full 3D modeling and mesh was generated for each case. All cases were simulated at the compressor maximum continuous speed, using its operating temperature and pressure. Table 2 presents the operating conditions and number of elements of each mesh.

**Table 2 – Number of mesh elements and operating conditions for each CFD case**

| | Case A | Case B | Case C |
|---|---|---|---|
| Number of mesh elements | 5,908,149 | 6,554,710 | 8,574,629 |
| Seal inlet pressure [bar(a)] | 187 | | |
| Seal outlet press. [bar(a)] | 57 | | |
| Temperature [°C] | 170 | | |
| Rotor speed [rpm] | 13920 | | |
| Inlet preswirl | 0* | | |

*Since swirl brakes are modeled.

*Solution Method*

The commercial software ANSYS CFX 14.0 was used to solve the Reynolds Averaged Navier-Stokes (RANS) equations. The *k-ε* standard model was used for the turbulence modeling because it shows good compatibility in the representation of turbulent flow with a reduced computational cost. Within ANSYS CFX 14.0, this turbulence model uses the scalable wall-function approach to improve robustness and accuracy when the near-wall mesh is very fine. The scalable wall functions enable solutions on arbitrarily fine near-wall grids, which are a significant improvement over standard wall functions (ANSYS, 2013). Isothermal flow model was adopted, since previous experimental studies from Childs and Wade (2004) have shown little change in temperature for hole-pattern annular seals. Also the gas compressibility was considered. A steady state solution was considered as initial step for the transient simulations. These initial steady state results proved extremely important for the convergence of the subsequent simulations because of the large differential pressure between the inlet and outlet of the seal, as shown in Table 2. Finally, to represent the periodic circular orbit of the seal center, a transient solution combined with mesh deformation was performed.

Using the values of Table 2, the boundary conditions at the inlet and outlet of the seal were defined as total pressure and averaged static pressure respectively. The stator was defined as a stationary no slip smooth wall, whereas the rotor wall, while also in the no slip smooth condition, moves in the *x* and *y* directions as described by Eq. (1), where Ω is the rotor synchronous precession, in rad/s, and *r* is the eccentric radius of the circular orbit described by the rotor, as shown in Fig. 6.

The forward and backward orbits were considered for each case, always with synchronous speed and a 15 *μm* eccentricity. According to the study of Moore (2003), the choice of eccentricity is arbitrary but is typically kept near 10% of the clearance to capture the linear, small motion characteristics. In this case, the eccentricity was selected to be 5% of the maximum clearance, in order to try to reproduce the excessive stiffness observed in the field for this damper seal. During simulations, the results of mass flow and resulting forces were monitored.

The simulations were performed in the operator's R&D Center existing clusters composed of Intel(R) Xeon(R) X5670 @ 2.93GHz processors. The number of processors used in each run varied from 12 to 48, with 24 Gb of RAM, according to the availability of each of them. Thereby, the minimum time required for a transient solution was of 4.4 hours for case A with 36 processors, and the maximum was of 18.5 hours for case B with 24 processors.

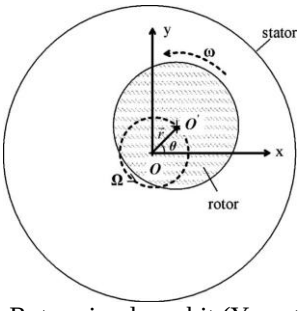


Figure 8 – Rotor circular orbit (Yan et al., 2011)

*Rotordynamic coefficients*

Yan et al. (2011) used the theory from Childs (1993) and the analysis method firstly used by Bolleter et al. (1987) to obtain the following relation between the rotordynamic coefficients and the forces on the rotor surfaces:

$$k = \frac{F_x^- - F_x^+}{2\mathrm{r}}$$

$$K = \frac{F_y^- - F_y^+}{2\mathrm{r}}$$

$$c = -\frac{F_y^- + F_y^+}{2\mathrm{r}\Omega} \qquad (2)$$

$$C = \frac{F_x^- + F_x^+}{2\mathrm{r}\Omega}$$

where the superscript "+" means forward orbit, the "–" means backward orbit, and $F_x$ and $F_y$ are the reaction forces in x and y directions, respectively.

*Results*

Figures 9 to 11 present the unsteady reaction forces in x and y directions from the CFD simulations of each case. It can be observed that, for all the simulations performed, the system reaches a periodic state right after the second oscillation period, therefore, the analysis can be performed considering the results after this time step.

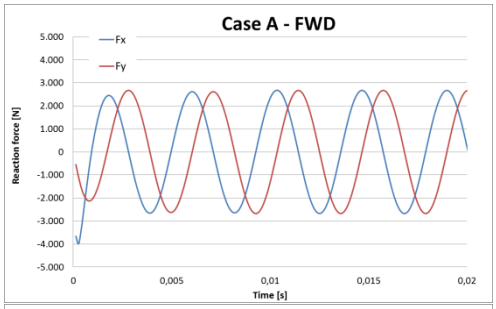


Figure 9 – Reaction forces from case A.

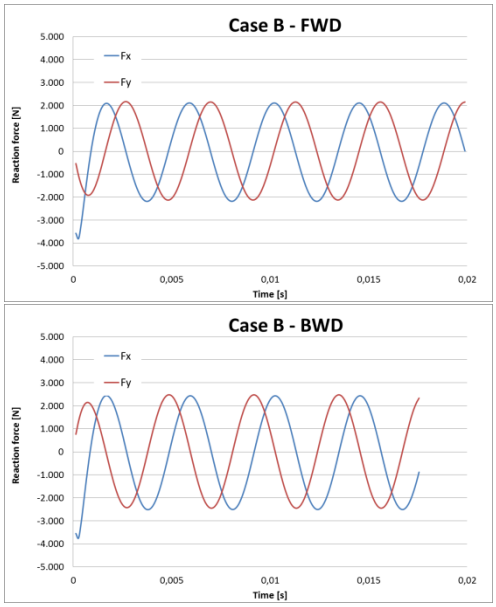


Figure 10 – Reaction forces from case B.

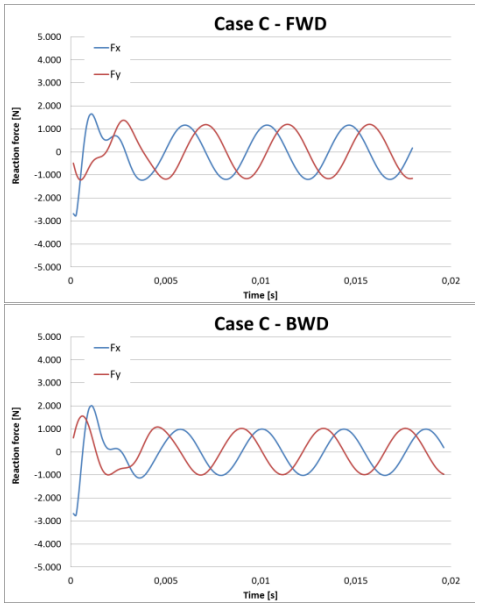


Figure 11 – Case C reaction forces.

It can be observed, from Figs. 9 and 10, that the magnitude of the forces induced by the flow in the annular seal is between 2000N and 3000N and that even the small change in geometry from case A to case B yields significant results in the magnitude of these forces, of over 500N for both forward and backward orbits. A severe reduction of the induced forces can be noticed in case C (approximately 50% when compared to the original geometry). It can also be noticed that the resultant forces in the backward precession are slightly lower than those of the forward precession, which is the opposite result as obtained from the two previous geometries.

Figures 12 and 13 show some of the pressure and velocity profiles resulting from the simulations. The seal leakage values are presented in Table 4.

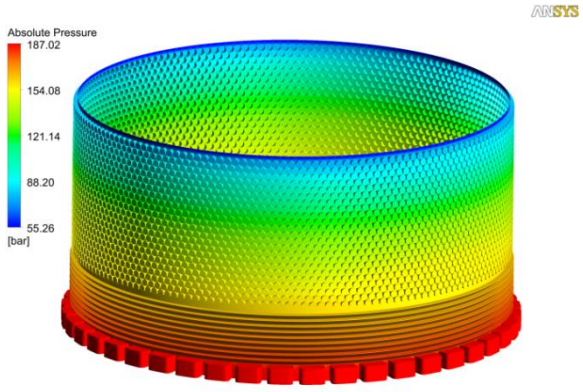


Figure 12a – Case A pressure distribution resulting from CFD simulations using operating conditions from Table 2.

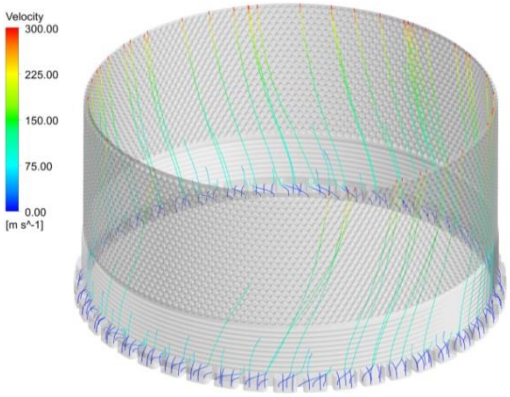


Figure 12b – Case A velocity profile resulting from CFD simulations using operating conditions from Table 2.

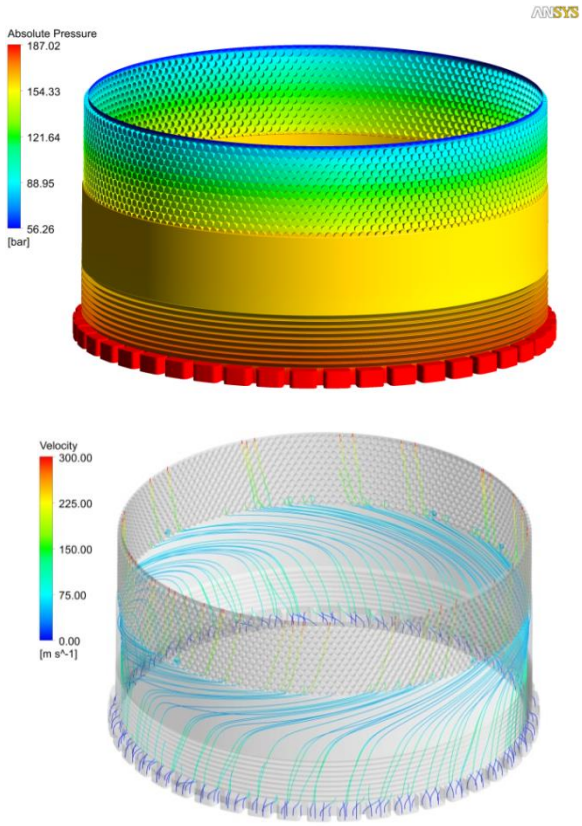


Figure 13 – Case C pressure and velocity profiles resulting from CFD simulations using operating conditions from Table 2.

## UNBALANCE RESPONSE AND STABILITY ANALYSES

The results obtained for the different configurations and by the two methods of calculation can be found in Tables 3 and 4.

For the cases "Seal & BP without Modification" and "Modification at Balance Piston", which were calculated through both methods, the differences in the dynamic coefficients are high (around two times for direct stiffness and direct damping and 6 times for cross-coupled damping in both cases), although there is good agreement in the seal leakage results. The difference between these results lies in the interaction between the different regions of the hybrid seal (labyrinth and hole-pattern for the case without modification and labyrinth/relief pocket/hole-pattern) that is captured by CFD but not by the individual bulk flow codes.

The coefficients in Table 3 were obtained through two independent simulations, one for the labyrinth and one for the hole-pattern, calculated using a bulk flow code with default values from the software for the empirical factors. Past OEM prediction on this seal informed the pressure curve shape along axial direction, thus enabling pressure relationship extraction which was used to estimate the intermediate pressure between the labyrinth and the hole-pattern regions. Due to the presence of swirl brakes, preswirl was supposed as 0.1 for the labyrinth and 0.5 for the hole-pattern seal.

**Table 3. Damper seal coefficients calculated through rotordynamic software**

| **Coefficient /Cases** | Rotor in operation | Without Modification (Case A) | Modification at Balance Piston (Case B) |
|---|---|---|---|
| **Direct Stiffness Kxx=Kyy (lbf/in)** | $3.272*10^5$ | $4.054*10^5$ | $2.603*10^5$ |
| **Cross-Coupled Stiffness Kxy=-Kyx (lbf/in)** | $3.302*10^4$ | $3.569*10^4$ | $3.083*10^4$ |
| **Direct Damping Cxx = Cyy (lbf.s/in)** | 207.3 | 187.0 | 220.6 |
| **Cross-Coupled Damping Cxy = -Cyx (lbf.s/in)** | -8.8 | -9.7 | -7.9 |
| **Leakage (kg/s)** | 1.64 | 1.42 | 1.85 |

**Table 4. Damper seal coefficients calculated through CFD**

| **Coefficient /Cases** | Without Modification (Case A) | Modification at Balance Piston (Case B) | Modification in Seal (Case C) |
|---|---|---|---|
| **Direct Stiffness Kxx=Kyy (lbf/in)** | $9.323*10^5$ | $6.279*10^5$ | $2.800*10^5$ |
| **Cross-Coupled Stiffness Kxy=-Kyx (lbf/in)** | $3.132*10^4$ | $2.125*10^4$ | $2.918*10^4$ |
| **Direct Damping Cxx = Cyy (lbf.s/in)** | 411.4 | 408.0 | 200.5 |
| **Cross-Coupled Damping Cxy = -Cyx (lbf.s/in)** | -60.9 | -47.4 | 50.4 |
| **Leakage (kg/s)** | 1.44 | 1.89 | 1.60 |

Using the coefficients obtained by CFD, damped unbalanced response and stability analyses were conducted. The most interesting results in the damped unbalanced response analyses are shown in Figure 14, which refers to vibration amplitude at the non-drive end due to unbalance placed at the first impeller from suction side, also near the non-drive end. For the operator, this is the most likely location to build up unbalance due to fouling. The curve in red corresponds to a simulation without seal effects and represents the compressor with the recycle valve open. The curve in green corresponds to seal & BP without modification. The difference between both curves at about 11,000 rpm reproduces what was being observed at the platform: when the recycle valve closes, the vibration in this side rises significantly, due to the rpm increase of the first critical speed. The curves in blue represent the two studied modifications, with the one corresponding to modification in the seal presenting a smaller sensitivity to unbalance in the operating speed range.

Proceeding to the stability analysis based on the CFD calculated balance piston coefficients and on the OEM´s procedure, as delineated on the original Lateral Analysis document, there was an indication that for the non-modified configuration the Log. Dec. would be at least 1.17, rising to 1.36 if the modification in the balance piston was applied and kept nearly constant with the seal modification, at about 1.15.

These values were above OEM´s predictions, which were based on damper seal coefficients calculated from the ISOTSEAL program.

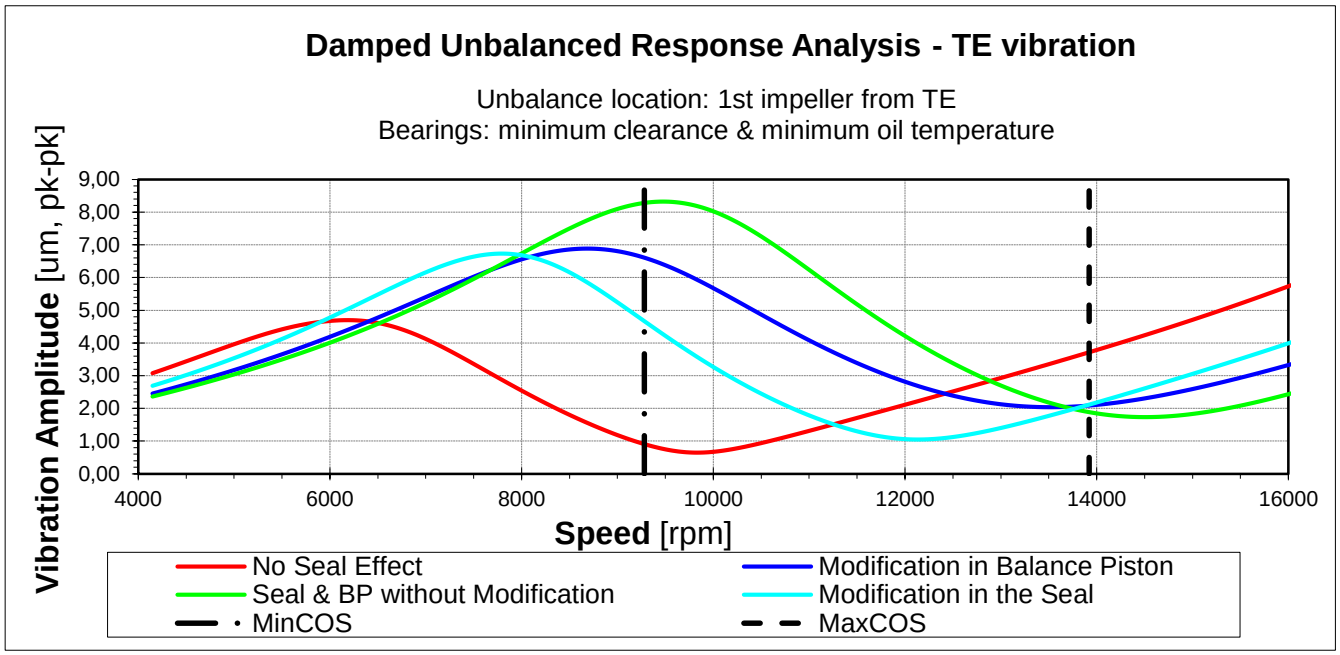


Figure 14 – Damped Unbalanced Response Simulations for Unbalance applied near NDE.

## FIELD BEHAVIOR

In a maintenance intervention where even CFD and rotordynamic analyses were employed, it is important to verify how effective the intervention was. This is documented by the following two figures. Fig. 15 shows the last 120 hours of operation with the old compressor bundle. At that time, the compressor was being used only for export service, with the discharge pressure limited to 140 bar (the export header pressure), with speed limited to 13,000 rpm and the recycle valve less than 50% closed. Nevertheless, the NDE vibration was around 80 microns (X sensor) and the machine reliability registry records 8 trips due to high vibration during these last five days of operation.

Fig. 16 shows another 120 hour period, recorded February 2014, with already seven months of operation with the new damper seal. The compressor is now aligned to the gas lift header, providing 186 bar of pressure. The speed is slightly higher, at 13,200 rpm and the recycle valve is fully closed. All four vibration sensors are below 15 microns. The compressor shows a highly stable operation behavior.

## CONCLUSION

When the operation of an offshore compressor degrades to a point of requiring the change of its internals, it is very important that this swap achieves a high level of effectiveness, which was not happening on this platform. The use of rotordynamic simulations based on CFD calculated annular seal dynamic coefficients made it possible to provide a substantial improvement on the dynamic behavior of this machine. It additionally provided an interesting example of the application of computational fluid dynamics on a maintenance issue.

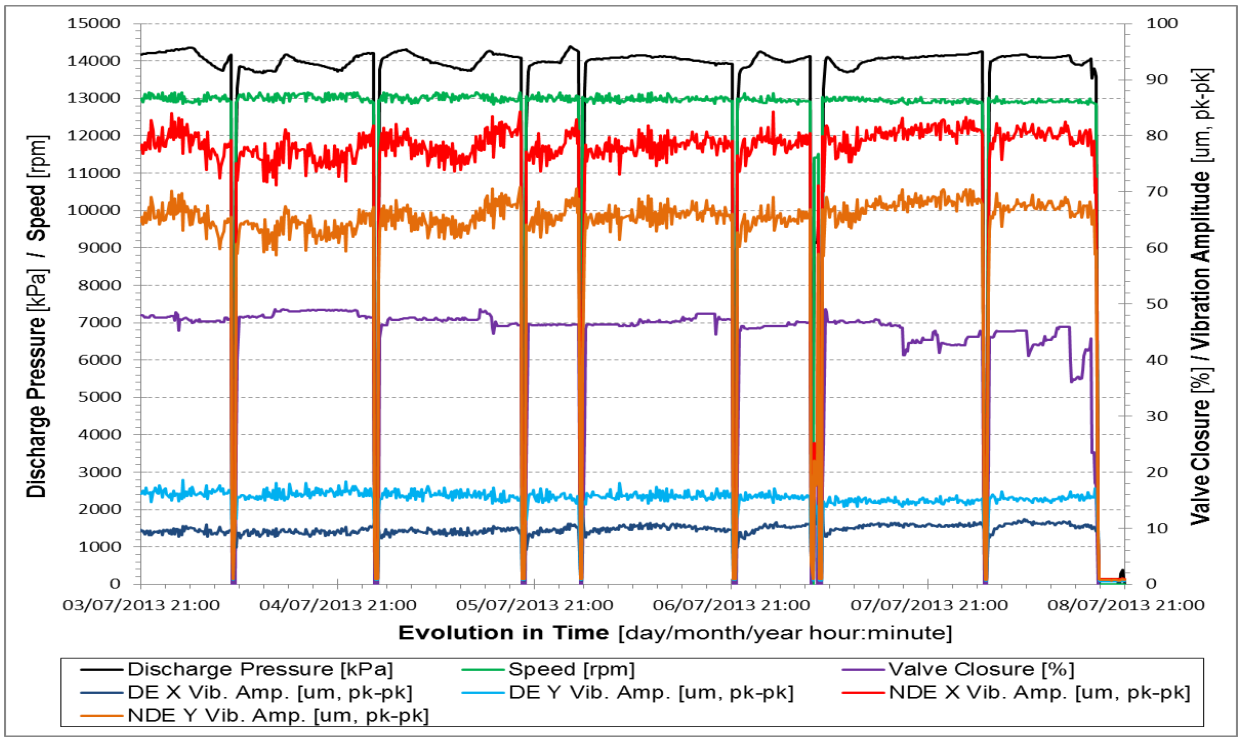


Figure 15 – Compressor behavior during the last 120 hours with the old bundle.

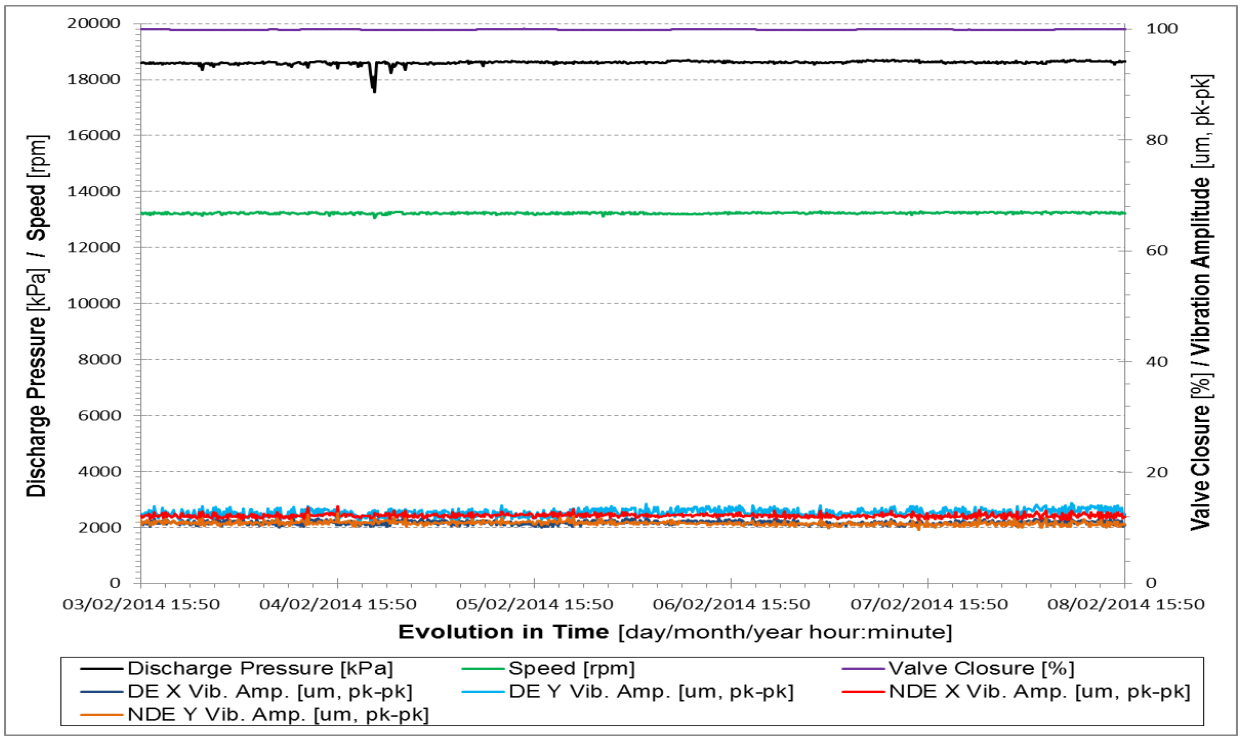


Figure 16 – Compressor behavior seven months after the bundle swap, also for 120 hours.

Nevertheless, this work faced some limitations, including the cooperation between Operator and OEM, which was mutually independent in its beginning, with the details of one approach being known by the other only when writing this paper. Hence, while the Operator considered, from measurement, that the original balance piston was completely tapered, the OEM considered that it was straight below the labyrinth seal and swirl brakes. These dimensional differences should not and, according to the results, did not give a significant error, since the dimensions on the hole-pattern part of the seal were dominant on the dynamic behavior of the seal. Another difference on approach was that the OEM, based on its experience, considered a central unbalance on its rotordynamic analyses, while the Operator, for equivalent reasons, considered unbalance on the first impeller.

The Operator has used CFD techniques to help diagnose two other cases of field problems and it is believed that in the future the use of numerical tools, such as CFD and FEA (Finite Element Analysis), to assist in solving turbomachinery operation and maintenance issues will increase. On the OEM side, internal design practices have been in place for many years now that include a check of the first critical speed location with seal effects included. This ensures the first critical speed is outside the planned operating speed envelope. Finally, this example also illustrates the importance of a cooperative work between equipment user and manufacturer on solving an operational problem.

## REFERENCES

ANSYS, 2013, ANSYS CFX User Document, Version 14.0.

Bolleter, U. et al., 1987, "Measurement of Hydrodynamic Interaction Matrices of Boiler Feed Pump Impellers", ASME J. Vib., Acoust., Stress, Reliab. Des., 109, pp. 144–151.

Childs, D., 1993, "Turbomachinery Rotordynamics: Phenomena, Modeling, and Analysis", Wiley-Interscience, New York.

Chochua, G. and Soulas, T.A., 2007, "Numerical Modeling of Rotordynamic Coefficients for Deliberately Roughened Stator Gas Annular Seals", ASME Journal of Tribology, Vol. 129, pp. 424–429.

Hirs, G.G., 1973, "A Bulk-Flow Theory for Turbulence in Lubricant Films", J. Lub. Technol., 95(2), pp. 137–145.

Kleynhans, G.F., and Childs, D.W., 1997, "The Acoustic Influence of Cell Depth on the Rotordynamic Characteristics of Smooth-Rotor/Honeycomb Stator Annular Gas Seals", ASME Trans. Journal of Engineering for Gas Turbines and Power, October 1997, Vol. 119, No. 4, pp. 949-957.

Kocur Jr., J.A. et al., 2007, "Surveying Tilting Pad Journal Bearing and Gas Labyrinth Seal Coefficients and their effect on Rotor Stability", 36th Turbomachinery Symposium, Houston.

Migliorini, P.J. et al., 2012, "A Computational Fluid Dynamics/Bulk-Flow Hybrid Method for Determining Rotordynamic Coefficients of Annular Gas Seals", ASME Journal of Tribology, 134 (2), p. 022202.

Moore, J. J., 2003, "Three-Dimensional CFD Rotordynamic Analysis of Gas Labyrinth Seals," ASME Journal of Vibration and Acoustics, 125, pp. 427–433.

XLTRC2, 2015, see site "turbolab.tamu.edu/trc/trc-membership-information/"

Yan, X. et al., 2011, "Investigations on the Rotordynamic Characteristics of a Hole-Pattern Seal Using Transient CFD and Periodic Circular Orbit Model", ASME Journal of Vibration and Acoustics, 133(4), p. 041007.

## ACKNOWLEDGMENTS

The authors would like to thank both PETROBRAS and Dresser-Rand for their support and permission to publish this work.